Research Article

Huaier Effects on Functional Compensation with Destructive Ribosomal RNA Structure after Anti-SARS-CoV-2 mRNA Vaccination

Manami Tanaka[1*], Tomoo Tanaka[1], Xiaolong Zhu[2], Fei Teng[2], Hong Lin[2], Zhu Luo[3], Ying Pan[2], Sotaro Sadahiro[4], Toshiyuki Suzuki[5], Yuji Maeda[6], Ding Wei[7], Zhengxin Lu[8]

Abstract

Although striking effects of vaccination strategy against COVID-19 world-wide, a long-term influence by sequential viral mRNA injections are unknown. We analysed biological alterations by total RNA sequencing in Pfizer-BioNTech vaccinated normal healthy volunteers and cancer patients, with or without adjuvant Huaier therapy. A significant destruction in ribosomal RNA structures was identified, enhanced by serial shots. Unlike the destruction caused by chemotherapy with platinum (II) complex, progressive destruction in 18S ribosome was identified even at 6 months after vaccination. The influence resulted in massive inhibition of translation and transcription, significantly in intra/inter neural signaling transfer and in lipid metabolism, related to ageing process. Huaier compensated these dysfunctions by miRNA-mediated transcriptional control, by typical activation in PI3K/AKT signaling pathway. Gene Ontology analysis revealed spontaneous virion production in number even after 3 months of the first vaccination. Present study indicated that the adjuvant therapy like Huaier compensates accelerated ageing process by mRNA vaccination.

Introduction

Because of pandemic SARS-CoV-2 infection, the most important transfer has been long perturbed in materials, personals, and information in need [1] Vaccination against the virus drastically improved the situation, however, the world has not yet reached a goal of this pandemic infection even by the third, fourth, or possible repetition of the vaccine injections in every generation [1-3].

On the other hand, there are an increasing number of reports everyday which might relate to a long-term influence of viral mRNA [4] injection besides the principal objective as anti-COVID-19 in Japan; for example, traffic accidents caused by loss of consciousness during driving, as well as cardiac and cerebral infarction because of increase of micro-embolism production in elderly population. Many Japanese population is genetically linked to hypertension and hyperlipidemia, and being generally treated by daily dose of medicines prescribed by walk-in clinics nearby for a life-long period5. Actually, it is rare to find the elderly population over 70 years old without any daily dose of medicine related to those disorders, together with anti-coagulant agent as preventive medicine against embolism.

Since Japanese population suffers more from neuro-degenerative diseases and disorders like Alzheimer's disease, chiefly caused as a result of longevity about 100 years of life, it is not so common to have as much sudden symptoms and accidents by thrombosis as recently reported [5].

In the course of our clinical research to investigate molecular basis of anti-cancer efficacy of Huaier [6-16], we happened to observe several patients suddenly deteriorated without any considerable factors. The patients with Huaier therapy maintained good quality of life (QOL) for more than expected by any means, and confirmed the recovery judged by any medical tests including CT and MRI images. We have identified cerebral embolism in the patients suddenly deteriorated, at shortest within one week of 2nd injection of anti-COVID-19 vaccine.

We thus initiated the clinical research to identify any possible molecular changes and/or alterations after mRNA vaccination, with consideration to Huaier therapy. We compared results in the cancer patients with a long history of Huaier therapy, to those obtained in normal healthy controls, with or without Huaier administration. We have paid special attention to the influence of vaccination to the system involved in the ageing process and neural signal transfer.

Affiliation:

[1]*Bradeion Institute of Medical Sciences, Kanagawa, Japan*

[2]*BGI-Shenzhen, Shenzhen, China*

[3]*BGI-Japan, Kobe, Japan*

[4]*Department of Surgery, Kameda-Morinosato Hospital, Kanagawa, Japan*

[5]*Department of Surgery, Oiso Hospital attached to Tokai University School of Medicine, Kanagawa, Japan*

[6]*Department of Surgery, Kanagawa National Hospital, National Hospital Organization, Kanagawa, Japan*

[7]*Japan Kampo NewMedicine, Tokyo, Japan*
[8]*QiDong Gaitianli Medicines Co. Ltd., Jiangsu Province, China*

*Corresponding author:
Manami Tanaka, Bradeion Institute of Medical Sciences, Co., Ltd., Itado 433-1, Isehara, Kanagawa 259-1145, Japan.

E-mail: tubu0125@gmail.com
manami-tanaka@bradeion.com

First significant observation soon after the first shot of Pfizer-BioNTech mRNA vaccination [4] was poor quality of extracted RNA. The ribosomal RNA structure changed drastically, and destructive changes seemed to result in the quantitative inhibition in the process of translation and transcription. This destructive influence became more and more prominent according to the serial vaccinations, even at 6 months after the first injection. These changes resulted in the broad inhibitory effects in numerous signaling transfer network. Huaier, however, successfully compensated possible dysfunction in biosystems by microRNA-mediated transcriptional control6, and the activation of PI3K/AKT kinase signaling pathway [12] was typical sign of recovery with abundant alterations in transcription factors. In addition, the inhibitory influence to intra/inter neural signal transfer was also recovered as symbolic to prevent accelerated ageing process [2] by the serial vaccinations., which directly or indirectly affected endocrine secretions.

It is noteworthy that the present study could demonstrate the virions and virion part were detected in number by Gene Ontology enrichment analysis. This is another proof to the reported facts [17] that the partial mRNA of the virus injected could spontaneously produce multiple virus copy in the recipients.

Thus, the present study succeeded to provide the clue to define a long-term influence of Pfizer-BioNTech mRNA vaccination against SARS-CoV-2 to Japanese population. The system affected was closely related to ageing process demonstrated in Alzheimer's disease cascade, lipid metabolism via apolipoprotein function [18, 19] in endothelial cells, and regulated by intra/inter neural signal transfer. These inhibitory effects of mRNA vaccines can be compensated by, for example, Huaier administration by miRNA-medicated transcriptional control [6], via an activation of PI3K/AKT kinase-related signaling pathway [12].

The present study shed lights into the preparation for era after COVID-19, i.e., by full support for vaccine strategy with Extended of kinase regulator as Huaier.

Methods

Sample collection and medical ethics policy

Blood samples were taken from 8 patients, two of them were healthy volunteers as controls. The clinical characteristics of patients like sex/age/cancer origin and prognosis are summarized in **table 1**. The present study was strictly conducted according to the guidelines of the *Declaration of Helsinki* and the principles of good clinical practice. Written informed consent was obtained from the patients. This clinical research was applied according to the *Consolidated Standards of Clinical Research Trials* guidelines and was registered on the Japanese Medical Association (ID: JMA-IIA00335, 1st February 2018). The project has been strictly conducted with a review by the ethics committee consisted by the experts on Medicine, Nursing, Laws, Pharmaceutics, and Business Community (first committee held on 9th February, 2018) [6, 9-15, 20].

Total RNA sample QC

The Agilent 2100 Bio analyzer (Agilent RNA 6000 Nano Kit) were used to do the total RNA sample QC. The QC Item contains the RNA concentration, RIN value, 28S/18S and the fragment length distribution.

Library and sequencing

The obtained peripheral blood samples (28 samples from 8 cancer patients) were designated to be further sequencing. First purifying the poly-A containing mRNA molecules using poly-T oligo-attached magnetic beads. Following purification, the mRNA is fragmented into small pieces using divalent cations under elevated temperature. After removal of rRNA, the RNA was converted into cDNA using reverse transcriptase and random primers. This is followed by second strand cDNA synthesis using DNA Polymerase I and RNase H. These cDNA fragments then have the addition process by A-tailing and the cDNA was amplified. To generate libraries, the amplified products were separated into single strand DNA and cyclized. The RNA-seq libraries were subjected and sequenced with the pair-end option using BGISEQ-500 system at Beijing Genomics Institute (BGI), China [6, 9-15, 21].

We have also performed total non-coding small RNA sequencing on the same platform. First, separate 18-30nt RNA segment by PAGE gel. And add ligation of corresponding adaptors to the RNA 5′ and 3′ ends, the adapter-ligated small RNAs were subsequently transcribed into cDNA, and amplified the product by several cycles. Then reverse extend the RT primer in next step to synthetize strand cDNA and use high-ping polymerase to amplify cDNA, enrich cDNA with both 3' and 5' adaptor. Purified DNA was used for cluster generation and sequencing analysis using the BGISEQ-500 platform.

Total RNA was isolated from the serum samples and was pooled together to construct cDNA Libraries. These libraries were subsequently sequenced throw Illumina HiSeq sequencing with pair-end reads of length 2* 100bp according to manufacturer's instructions as previously described [6, 9- 15, 21].

Data process and expression analysis of RNAseq

The sequencing data were analyzed and filtered using software soapnuke [22]. Clean reads were mapped to the human reference genome GRCh38 with software bowtie2. Then, the gene expression level of each sample was calculated using RSEM [23]. The expressed genes were further analyzed between the groups were detected by software DESeq2 [24], the significant differentially expressed genes (DEGs) were defined with fold-change lager than 2 and p-value smaller than 0.05.

Data process and expression analysis of miRNA

Low quality sequencing data were removed at first, and align the reads to miRbase database with bowtie2 [25] and calculated the expression level of miRNAs which standardized by TPM. Differentially expressed miRNAs between two samples were screened out strictly based on Poisson Distribution. Then, we make multiple hypothesis test correction for the p value of difference test, and to judge the significance of gene expression difference, FDR≤ 0.001 and the absolute value of $Log_2Ratio≥1$ are set as the default threshold. Software miRanda [26] and TargetScan [27] were used to get the target gene of differential expressed miRNA and extract intersection or union of target gene as final prediction result.

Functional analysis of target genes and DEGs

And to determine the metabolic and signal transduction pathways and their biological functions. Pathway enrichment and GO significance enrichment analysis was performed on the target genes of differentially expressed miRNAs or DEGs by using R package 'phyper'. For each P-value, we correct for multiple comparisons by controlling the False Discovery Ratio. And the terms for which the FDR was not greater than 0.01 were defined as statistically significantly enriched.

Results

Patient characterization

The medical characteristics of total 8 volunteers, 6 patients and 2 normal healthy control, with sampling times were summarized in **Table 1**.

Table 1: Clinical features of cancer patients and normal controls.

Number of patients or healthy controls	1	2	3	4	5	6	7	8
Age	67	54	76	56	67	81	67	77
Gender	M	M	M	M	M	F	M	F
Diagnosis	healthy control	heathy control	prostate cancer in situ, oesophageal cancer	pancreas cancer	colorectal cancer	colorectal cancer	lung cancer	oesophageal cancer
Stage			I	IV	IV	III→IV	IV	IV
Metastasis			not detected	lung, liver	both lung (multiple), peritoneal	liver (multiple),peritoneal	pleural effusion, thorax	both lung (multiple), adjacent lymph nodes
Huaier Administration	none	6 g / day	20 g / day → 60 g / day	60 g / day	20 g / day	20 g / day→none	60 g / day → 40 g / day	20 g / day→ none
Duration of Huaier therapy		3 years	3.5 years	2 years	2.5 years	1.5 years	8 months	1.5 years
Blood sampling time								
1. Before vaccination	○	○		○	○	○		
2. 3 weeks(before 2nd vaccination)	○	○				○		
3. 6 weeks	○	○		○		○		
4. 12 weeks (3 months)	○	○	○		○	○		
5. 4 months			○					
6. 6 months	○	○	○	○	○		after 2nd shots	after 2nd shots
7. 9 months (before 3rd vaccination)	○	○		○			○	○
8. 9months + 3 weeks after 3rd vaccination	○	○		○			○	
9. 3 months after 3rd vaccination	○	○	○	○			○	○
Complication	not specified	not specified	hyperlipidemia	not specified	not specified	abdominal pain, appetite loss, constipation, anemia, anorexia	anorexia	dysphasia
Additional treatment	none	none	none	surgical dissection before Huaier tr.	surgical dissection and FOLFOX tr. before Huaier tr.	none	none	none
Prognosis	healthy	healthy	complete remission	remission	complete remission	remission→relapse after vaccination→deceased	remission	remission→relapse after vaccination→deceased

The mean age is 69 years old, since this research excluded the congenital cancer or tumor. Huaier (*Trametes robiniophila murr*) has been recognized widely as anti-cancer drug in China (Chinese administration license No. Z-20000109) and provided as granule form from the manufacturer [6] The mRNA vaccine against SARS-CoV-2 used in the present study was Pfizer-BioNTech COVID-19 vaccine [4]. The sampling period was from April to December 2021. In these periods, the alpha, delta to omicron SARS-CoV-2 strains were simultaneously detected, and mixed especially in Tokyo, Japan.

The present study summarizes the results of RNA sequencing from 28 samples of those 8 volunteers. The sampling time was clearly indicated as ○ matched to the serial vaccination schedule. Because of the difficulty of material transfer from Japan to China, the analysis on the samples at 6 months after 3rd vaccination was not yet performed (indicated by ○). These results will be shown in another report in near future. The cancer patients have continuous Huaier administration, and prognosis was maintained in very good status as reported previously (patients No.3 described in the reference 14, No. 4, 6, and 8 in the reference 13). Since the vaccine program was scheduled by the local administrative office, we could not organize the sampling schedule for the present study, unlike in the case in normal healthy controls. patients No. 4, 5, 7, and 8 has not finished 3rd shots yet, but months have passed after 2nd shots in patients No. 7 and 8. None of the patients were detected COVID-19 positive during the research period, or no symptoms of infection. The observed side effects of the vaccination were the usual pain at the arm spot by the shot, slight fever ($< 37.5℃$), headache, fatigue, *etc.*, which were commonly reported, lasted about 24- 48 hours. The patient No. 6 and 8, in a very good remission stage as reported, suddenly detected deteriorated, and deceased soon after the final vaccination. There were no significant factors for this poor prognosis during over years' time course of Huaier treatment. Later, the mild stroke of cerebral infarction was detected in these patients. It is emphasized that the patient No.8, after 1.5 years of Huaier treatment, stopped Huaier administration 3 months before the first shot of Pfizer-BioNTech mRNA vaccination. The other patients had continuous Huaier administration for years as shown in **Table 1**. No patients have ever showed the symptoms or disorders related to hypertension, heart disease, cerebral thrombosis.

In the present study, we described sample number by patient No. and the timing of the samples, just as noted in the left side of sampling schedule (such as 1-1; patient No. 1, before 1st vaccination).

Destructive ribosomal RNA structures identified after serial vaccinations

Total 28 blood samples were analysed and provided the quantitative (about 7.0 GB RNA sequencing per each sample) and qualitative (mean number of 28,960 transcriptomes) genomic information. The results exhibited dynamic alterations amongst genome-wide transcriptomes, with average mapping ratio with reference genome is 76.33 % (ranging from 71.70% to 80.93%); 33,185 total genes were identified, and after the genome mapping and Gene Ontology classification, we defined 5,151 novel transcripts (**Extended Table 1**).

At the time of RNA extraction, first stage, we evaluated quality of extracted RNAs to determine whether to proceed to the following procedures by using Agilent 2100 [15, 20]. We have checked and quantified RNA concentration, 28S/18S & 23S/16S ribosome structures, and RNA integrity number (RIN) or RNA quality number (RQN) values for further library construction. **Fig. 1** demonstrate the ribosomal RNA structures observed throughout the research period. Unlike the past qualification results [9-15] the many samples in the present study were evaluated as risky or unqualified for further process (**Fig. 1**, left column in each patient

panel). Surprisingly, there identified 5S peak on the high side, which affects the quantitative inaccuracy and conduce to the inaccuracy of loading amount and the poor data quality. The RIN or RQN values were slightly under standard, too, with the same poor quality of 28S/18S or 23S/16S values evaluated also as under standard. Fortunately, all the samples were designated to proceed for further analysis and library construction, however, the destructive poor quality ribosomal RNA structures could not be fully recovered. Without Huaier administration (patient No. 1), progressive destructions were identified, with the excessive 5S peak and the decrease in 18S ribosome RNA peak were latent even at 6 months after the 2nd shots. These observations were common to the other patients (No. 2-7), detected as a long-term influence of serial mRNA vaccinations. The extreme damage, disappearance of the possible 28S ribosome peak was detected in the patient No. 8, total collapse of 28S ribosome structure in the last sample seems symbolic to the limits of genomic possibility and ability to recover from the disease. These observations have never been reported in the samples without vaccinations as reported previously in the patient 8 [15].

Summary of sequence results and RNA editing events

We identified total 2,712,591 SNP variant types in 28 sample analysis, and 96,878 single nucleotide polymorphism (SNP) per sample in mean number (ranging from 74,844 to 146,968), whereas 22,688 in total among normal healthy individuals [21] without Huaier or mRNA vaccine (**Extended Table 2**). The significant increase of total SNP numbers was consistent with the former reports. It is surprising that the maximum number was identified in normal individual (patient No. 1, without Huaier administration), 6 weeks after first vaccination, and the minimum number in patient No. 7, after 6 months of 2nd shots. As for the SNP variations, $A^*G > C^*T(I)$ transitions were the most common mutations (1,003,791and1,005,075, respectively, 74.1%), followed by, $C^*G>G^*T(I)$ (240,669 and 176,415, respectively, 15.4%) transversions, and $A^*C>A^*T$ (I) (173,930 and 112,711, respectively, 10.6%) transversions, which is much different from the previous reports on hepatocellular carcinoma [28] and oesophageal squamous carcinoma cells [29]. Mean number of transitions per sample is 71,745 (ranging from 55,805 to 105,628), whereas 25,133 transversions (ranging from 19,039 to 41,339).

The incidence ratio of transition was three times higher than transversion, which is much higher than that identified in oesophageal squamous carcinoma cells, breast cancer cells, and other cancer cells analysed before [6, 9-15]. It is obvious that the vaccination did not affect the genomic flexibility and capability observed in the former results [15].

SNP variations and incidence ratio drastically increased in number just as the same as Huaier treatment on cancer patients. but, in a different manner. Distribution of SNP and insertion or deletion of bases (INDEL) location showed no significant changes, either (**Extended Table 3**). Changes in relative abundance of isoforms, regardless to the expression change, indicates a splicing-related mechanism. We detected five types of alternative splicing (AS) events, including skipped exon (SE), alternative 5' splicing site (A5SS), alternative 3' splicing site (A3SS), mutually exclusive exons (MXE), and retained intron (RI). Approximately total 799,929 splicing events in 28 samples were observed, in which were 467,877 SE (58.5%); 75,594 MXE (9.5%); 76,1650 A5SS (9.5%); 92,511 A3SS (11.6%); and 87,797 RI (11.0%), respectively. Mean numbers of each event per sample (= per person) were 16,710 (ranging from 11,648 to 20,222) SE; 2,700 (ranging from 1,704 to 3,368) MXE; 2,720 (ranging from 2,156 to 3,003) A5SS; 3,304 (ranging from 2,756 to 3,567) A3SS; and 3,136 (ranging from 2,809 to 3,311) RI, respectively.

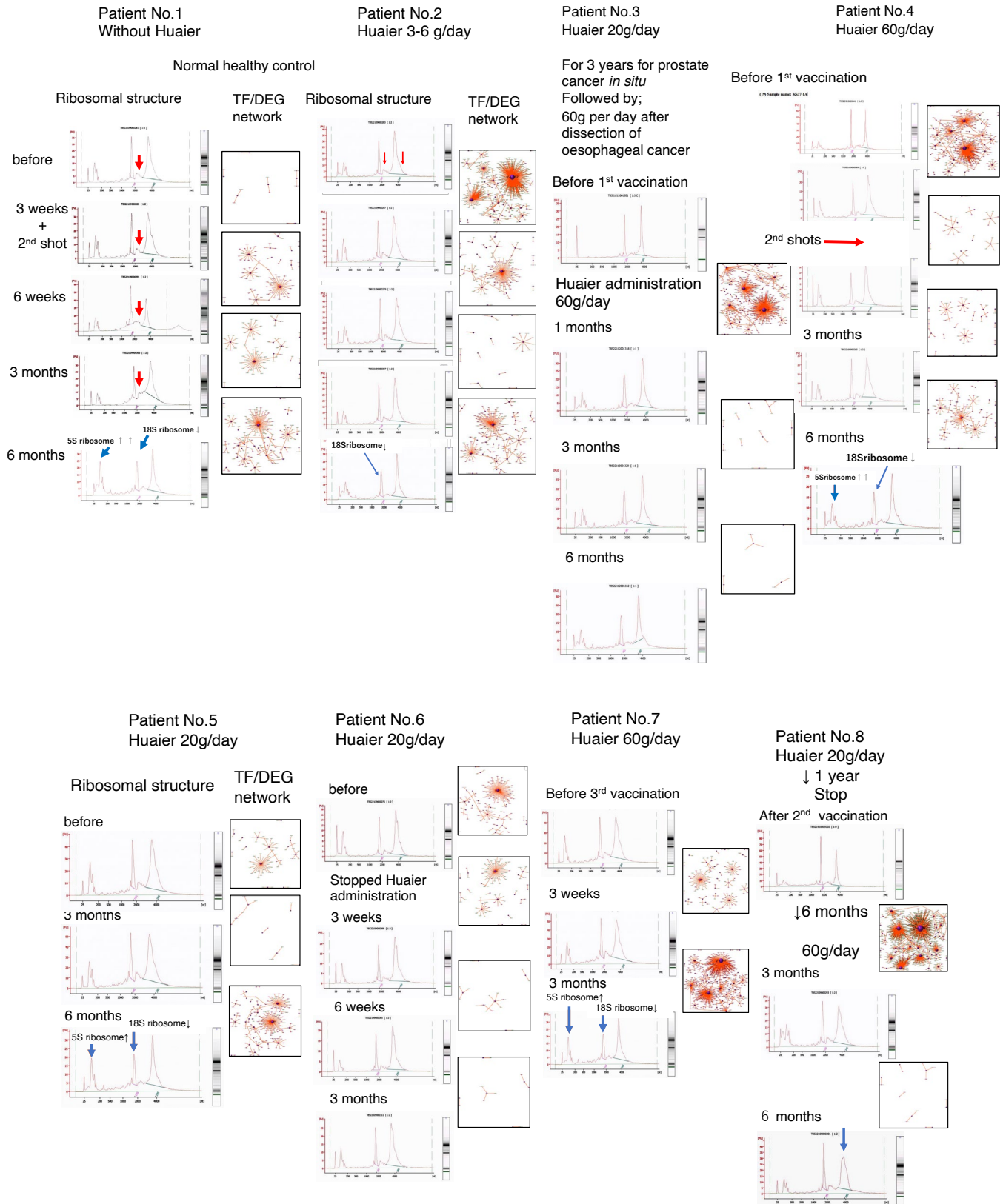**Figure 1:** Ribosomal structures by HPLC analysis with TF-DEG network in each patient by the time course of Pfizer-BioNTech vaccination. Left column: Ribosomal structures. Right column: TR-DEG predicted network. The red and green dots represent the up-regulated and down-regulated DEGs, respectively. Purple ball represents transcription factor, and the greater the node the more DEGs the transcription factor regulate.

A significant decrease in number of transversions in patients No. 5 and 7 (**Extended Table 2**, and isoform frequency (**Extended Table 3**) was identified at 3-6 months after 2nd vaccination in patient No. 5 were detected. The patient No.5 deteriorated suddenly after the 2nd shots of vaccination, and presented symptoms of mild stroke of cerebral infarction, such as memory loss, dizziness, paralysis, dysphagia, dysphonia, *etc*. The results obtained in the present study showed significantly high incidence in RNA editing events such as SNP and INDEL, approximately 4 times higher movability of the genome, ranging 2 times to 7 times higher compared with the normal individuals before 2019, without necessity of anti-COVID-19 vaccination.

The statistics of splicing events expanded the plasticity and flexibility inside the whole genome, and the enormous amount of the genomic capability to manage or cope with the extrinsic stimulus. The importance of these results will be discussed later.

Based on the expression information, we performed box plot to show the distribution of the gene expression level of each sample, followed by producing the density map which revealed the change of gene abundance according to the time course of the patients 9-15 (details were provided at BGI database).

Differentially expressed genes (DEG)-transcription factor (TF) network analysis

As a result of those analysis, gene expression level analysis enabled us to compare the levels of differentially expression genes (DEG) among samples (**Fig. 2**). The dynamics of these transcriptomes were monitored ty the time course of vaccination schedule described in **Table 1**. The

average number of up-regulated genes were 270 out of the total 19,762 transcripts (ranging from 9 to 1,712), whereas down-regulated genes were 237 (ranging from 5 to 1,095) (**Extended Table 4**). These numbers were significantly lower than those observed in Huaier-treated cancer patients before COVID-19 pandemic in the previous reports [6, 9-15]. In addition, more inhibitory, down-regulation of transcriptomes were overwhelmed than the numbers of up-regulated ones (**Fig. 2**). Such silencing effects on DEG should be estimated as the effects of mRNA vaccination, compared with the various types of Huaier therapy on cancer patients and normal controls in the former reports [15].

We analysed the links of those DEGs relationships with encoding transcription factors (TF). Total 2,216 DEGs coding transcriptional factors were altered to rescue and/or modify transcriptional misregulation (about 75 per sample), which is almost equivalent to 7,664 for 98 samples in the previous study (78 per sample) [15]. The results of the changes of TF-DEG network (results of comparison between two samples) clearly demonstrated in **Fig. 1** indicated significantly low and inhibitory effects in DEG dynamics after vaccination, together with the results in **Fig. 2**. The red and green dots in the figure represent the up-regulated and down-regulated DEGs, respectively. Purple ball represents each TF as a core. The greater the core size, the more DEGs regulated by the core transcription factor.

Although drastic activation of TF-DEG network like eruption observed before vaccination (in the patients 2, 3, 4, and 8), sudden silencing of network is prominent in almost all the samples, especially in the patient 8. Only exception was patient No.7, sudden increase in DEGs
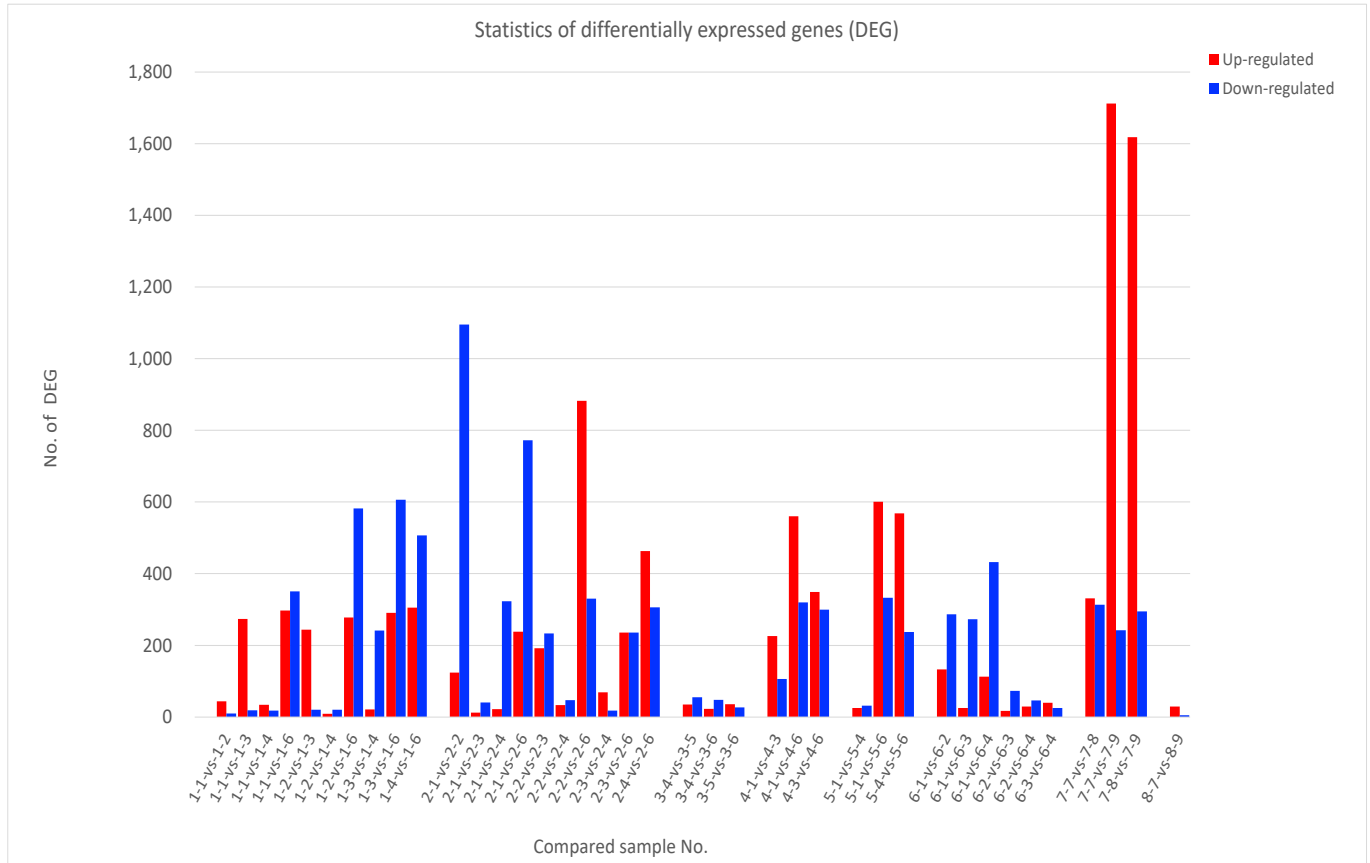
Figure 2: Comparison of the numbers of differentially expressed genes (DEGs) in each patient by time course of Pfizer-BioNTech vaccination.

Citation: Manami Tanaka, Tomoo Tanaka, Xiaolong Zhu, Fei Teng, Hong Lin, Zhu Luo, Ying Pan, Sotaro Sadahiro, Toshiyuki Suzuki, Yuji Maeda, Ding Wei, Zhengxin Lu. Huaier Effects on Functional Compensation with Destructive Ribosomal RNA Structure after Anti-SARS-CoV-2 mRNA Vaccination. Archives of Clinical and Biomedical Research 6 (2022): 553-574.

after on month of Huaier administration, who demonstrated significant recovery. This is the same as observed in the former report, the results caused by drastic ability of genomic potential evoked after a comparative large dose of Huaier.

So here we have another question, if the significant low degree of TF-DEG network changes in **Fig. 2**, how the possible damage from destructive ribosomal RNA structures, which might affect translational and transcriptional processes, can be restored, and maintained? Of course, we remember the genetic potential observed in the drastic increase in SNP/INDEL variants and total abundance of isoforms described above, we should identify how and why silenced TF-DEG network could recover the damages.

KEGG pathway classification on the influence of mRNA vaccination against SARS-CoV-2

With quantitative analysis of DEGs, we performed KEGG pathway classification (https://www.genome.jp/kegg/) to define the detailed mechanism after vaccination [30].

Figs. 3 and 4 demonstrate how biophysiological functions were maintained at 3 months after the first vaccination (9 weeks after 2nd vaccination), even with the destructive ribosomal RNA structures causing deficient translation. Panel a (patient No.1) showed the almost all the genetic alteration in transcriptional factors in normal individual, without Huaier administration. The resulting transcripts were kept normal as a result, which indicates no malfunctions in the major transcripts. Surprisingly, patient No. 1 was revealed to possess no point mutations nor genetic alterations in major oncogenes and tumor suppressor genes, which is the first case found in our clinical research.

Panel b, in normal individual (patient No.2) with 3-5g Huaier treatment for health maintenance, showed additional up-regulation of altered transcriptional factors for functional recovery, especially related to the endocrine secretion systems. In contrast, the failure of functional compensation was typically demonstrated in panel c (patient No.8). Even though genetic alterations in transcriptional factors were observed, the transcripts were down-regulated and functional genes were not activated.

Panel e-h further indicated the definite system for functional compensation. PI3K/AKT kinase-regulated signaling pathway [31-36], reported to be responsible for regulation of ribosomal RNA synthesis, showed significant relationship to the compensation mechanism to function recovery in those patients. With or Without Huaier administration, restoration and activation of phosphatidylinositol-4,5-bisphosphate 3-kinase (PI3K) and AKT kinase designated the maintenance of normal cellular signaling networks. Massive inhibition and down-regulation of related factors resulted in the poor prognosis in the patient No. 8, once had complete remission after 1.5 years' Huaier administration (20g/day) before vaccination.

The same was true in **Fig. 4**, lipid metabolism were analysed by KEGG analysis on Alzheimer's disease cascade. The up-regulation of APP (apolipoprotein) [18, 19] and ApoE [37-39] (apolipoprotein E) controlled good maintenance of lipid metabolism, and designated to compensate for the accelerated ageing process. Patient No.1 were prescribed Lipitor for hyperlipidemia. patient No.8 had relapse of oesophageal cancer13, together with suspected microembolus in the brain with the symptoms of memory loss, hoarseness, dysphagia, *etc.* The additional information related to inter/intra neural signaling cascade was shown in **Fig. 4**, panels e to h. As shown in **Fig. 3** panels e to h, the activation of neural signal transfer should be closely related and required for increased endocrine secretion in

the peripheral organs. Compared with results in **Fig. 3**, **Fig. 4** confirmed and highlighted the efficacy of Huaier administration to maintain the damaged functions after mRNA vaccination via destructive ribosomal RNA structures. The defects in lipid metabolism and neuro-degenerative factors seemed to be the cause of disorders appearing as a long-term influence after mRNA vaccination.

There were no significant changes in transcriptomes and factors related to RNA polymerases as reported previously in the present study (data not shown).

Alterations of small nuclear RNA expression

In the present study, simultaneously small non-coding RNAs (sncRNA) were sequenced using BGISEQ-500 technology [15, 20]. The statistics of detected small non-coding RNA (DSGs), miRNAs were shown in the upper panel of **Fig. 5**, panel a (upper panel), and piRNAs in panel b (lower panel) throughout the research period. No altered siRNAs were identified in the present study. The detailed numbers of each sample were summarized in. **Extended Tables 5** and **6.** The significant and drastic increase of down-regulated DESs (blue-bars) were matched with the significant alterations in transcriptional factors (total 2,216) as noted before. However, many miRNAs had no significant and meaningful relations to specific samples, both in the known and novel sequences (numerous amounts of data provided on requests) [40].

There were no specific miRNAs and piRNAs related to destructive ribosomal RNA structure production. Massive down-regulation DSGs were typical observation even in the cancer patients as well as normal healthy control with Huaier administration. It seems that these effects were not dependent on a dose, unlikely to the dose-dependent efficacy of Huaier. In patient No,7, highest numbers of down-regulation of DSGs were observed, whereas highest numbers of up-regulated DEGs contributed to accelerate cancer recovery.

These alterations in miRNAs were closely related to transcriptional factor chances as shown in **Fig. 3** panels a to d, which might contribute to decrease the damage and disfunction caused by destructive ribosomal RNAs.

Detection of quantitative virion and virion particles

Based on the significant DEG and KEGG pathway annotation [30], **Fig. 6** showed the pathway classification and functional information contributed to the expression changes. The pathway and process enrichment analysis has been carried out with the following ontology sources: KEGG pathway, GO biological processes [20].

Fig. 6 revealed up- and down-regulation of virion and virion particle production in the patient samples. In each panel, the numbers detected were described (indicated by *). Huaier clearly down-regulated the production of virion particles spontaneously appearing even at 3 months after vaccination. In panel a, the up-regulated virion production was silenced at 6 months after 2nd injection. Recently spontaneous production of virus copies after vaccination has been reported [17], and the preset study confirmed the fact in number. We could not define the process of virion production by intramuscular injections of virion part mRNAs, and that no COVID-19 infection was identified by common tests during research period so far. The further information obtained 6 months after 3rd vaccination will follow.

Although we can speculate that the presence of those spontaneously produced virion particles could contribute to ribosomal RNA structures, the reason why these destructive effects can occur and the mode of production still remains unknown.
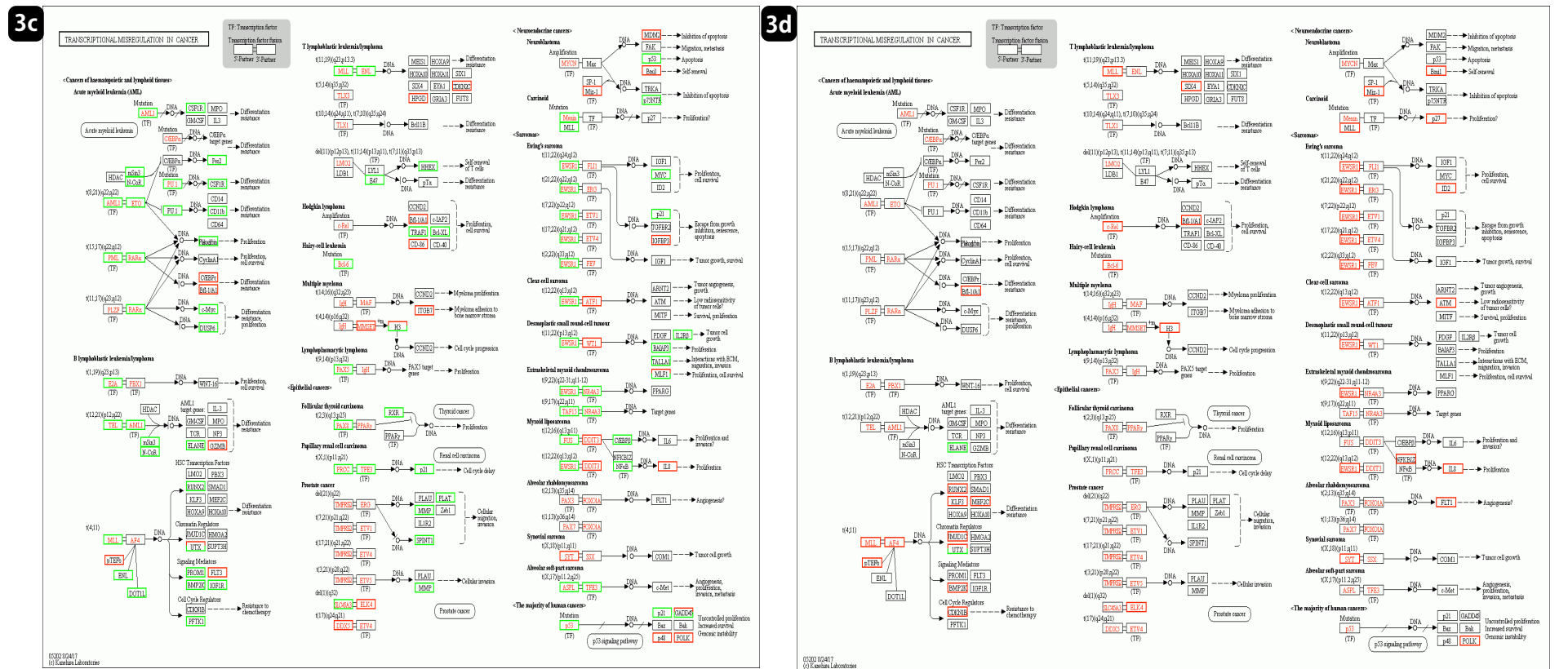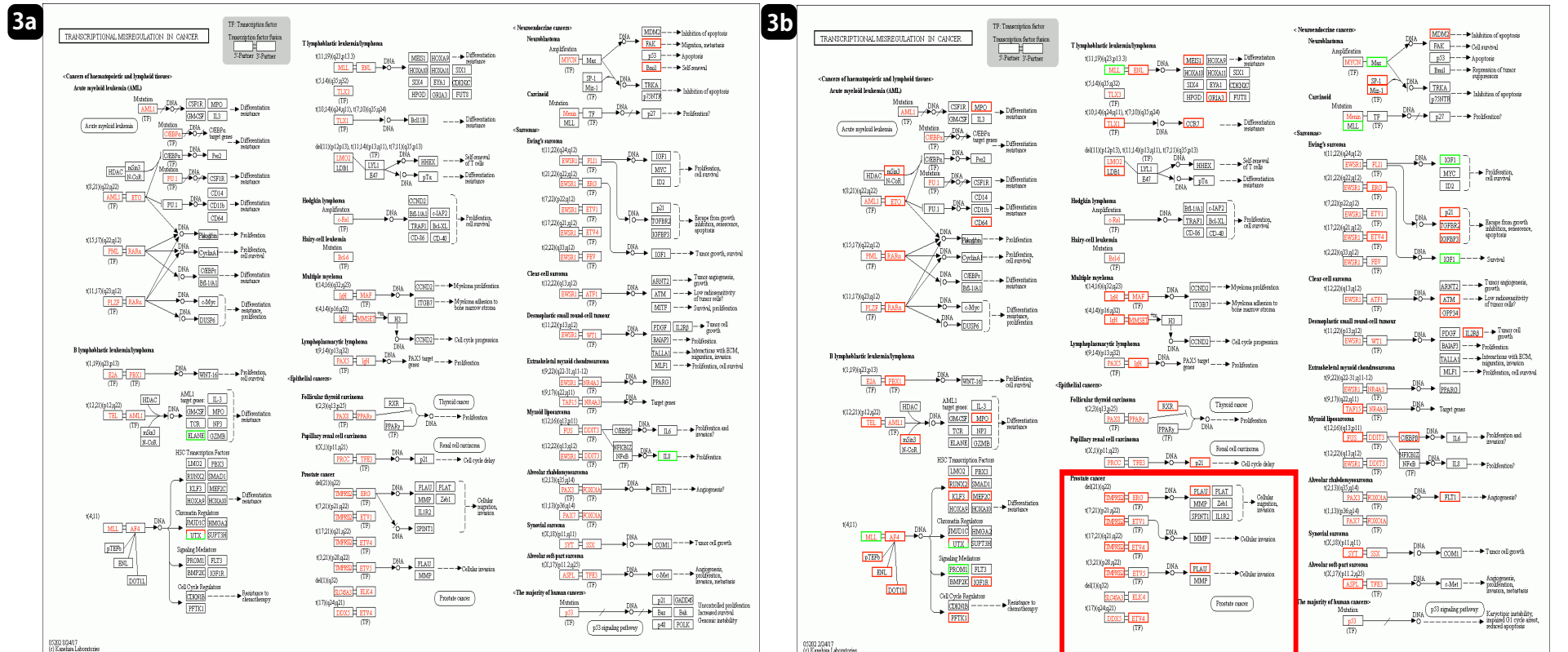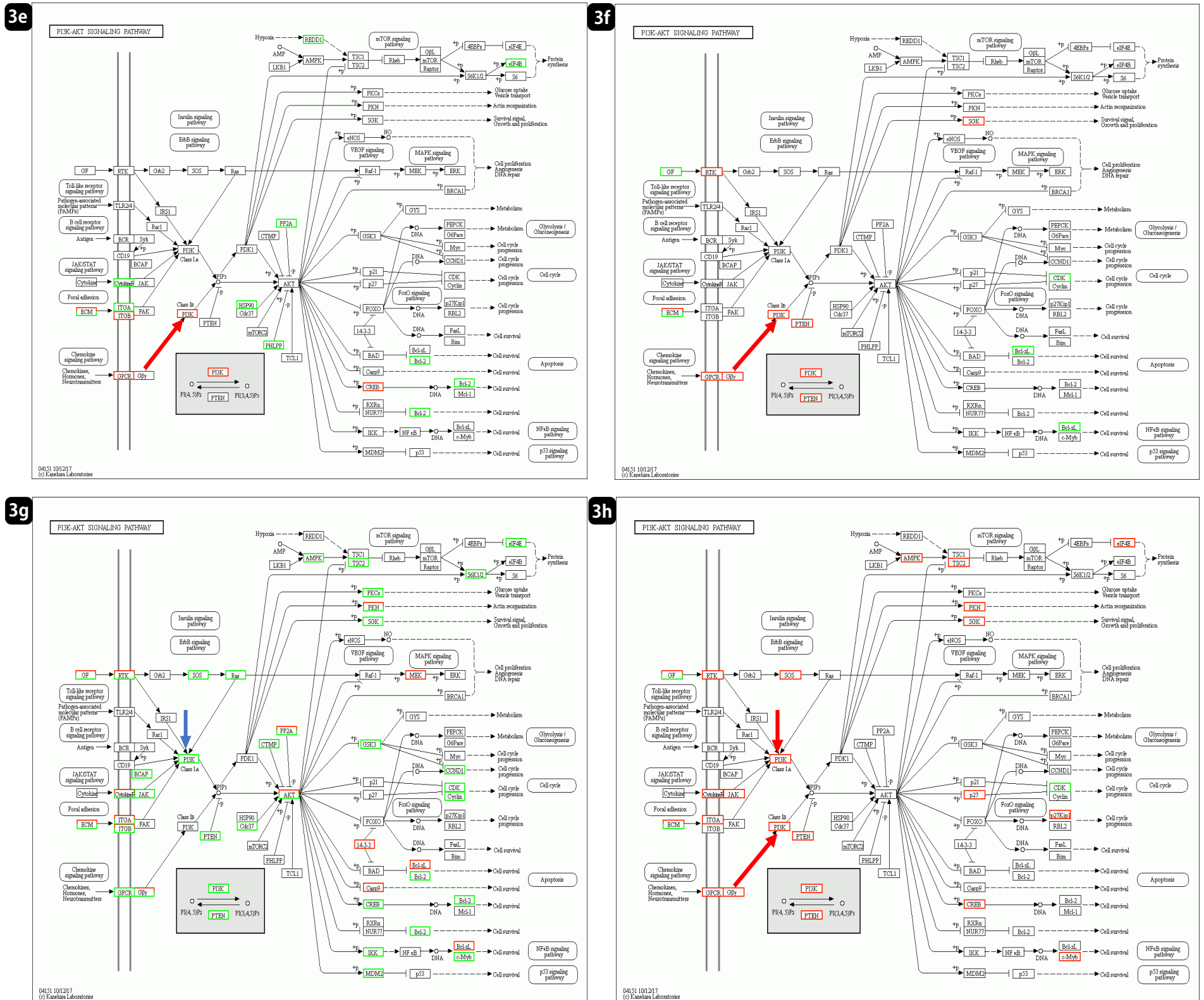
Figure 3: KEGG pathway analysis on transcriptional misregulation and P13K/AKT signaling pathway. a-d: KEGG panel on transcriptional misregulation. e-h: KEGG panel on P13K/AKT signaling pathway. a & d: patient No. 1; normal healthy control without Huaier administration. b & e: patient No. 2; normal healthy control with daily dose of Huaier 5g. c & f: patient No. 8; Stage IV oesophageral cancer, once successfully recovered, and relapse detected after 3rd shot of Pfizer-BioNTech vaccination. d & g: patient No.7; Stage IV lung adenocarcinoma, Huaier therapy 60g/day.

Citation: Manami Tanaka, Tomoo Tanaka, Xiaolong Zhu, Fei Teng, Hong Lin, Zhu Luo, Ying Pan, Sotaro Sadahiro, Toshiyuki Suzuki, Yuji Maeda, Ding Wei, Zhengxin Lu. Huaier Effects on Functional Compensation with Destructive Ribosomal RNA Structure after Anti-SARS-CoV-2 mRNA Vaccination. Archives of Clinical and Biomedical Research 6 (2022): 553-574.

Citation: Manami Tanaka, Tomoo Tanaka, Xiaolong Zhu, Fei Teng, Hong Lin, Zhu Luo, Ying Pan, Sotaro Sadahiro, Toshiyuki Suzuki, Yuji Maeda, Ding Wei, Zhengxin Lu. Huaier Effects on Functional Compensation with Destructive Ribosomal RNA Structure after Anti-SARS-CoV-2 mRNA Vaccination. Archives of Clinical and Biomedical Research 6 (2022): 553-574.
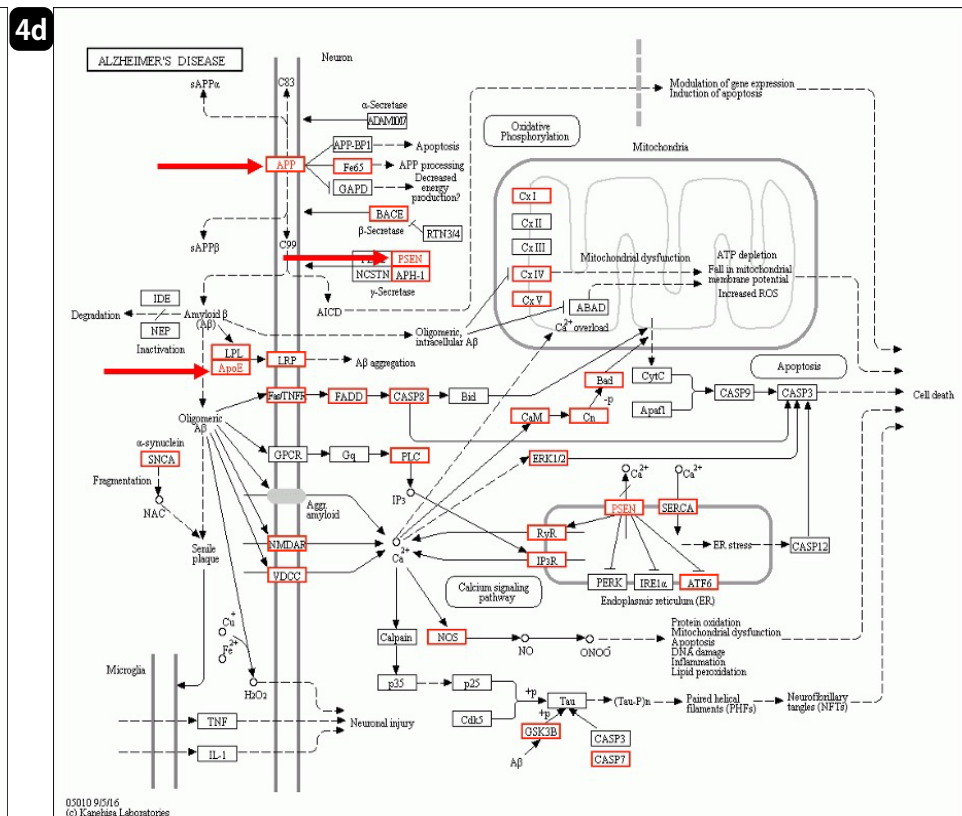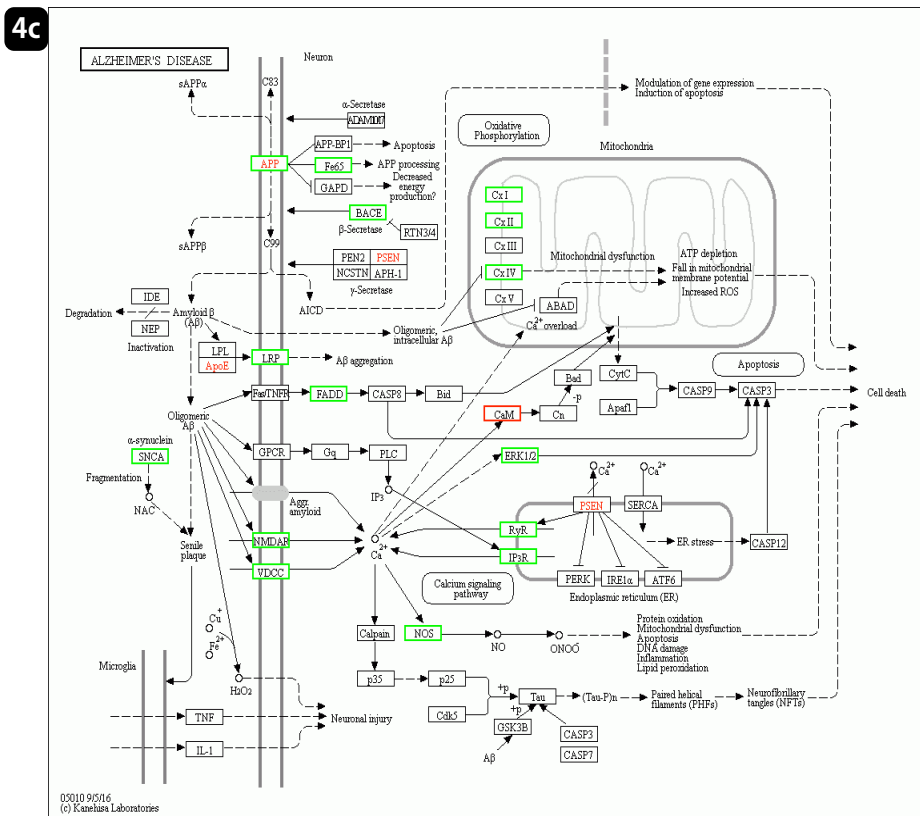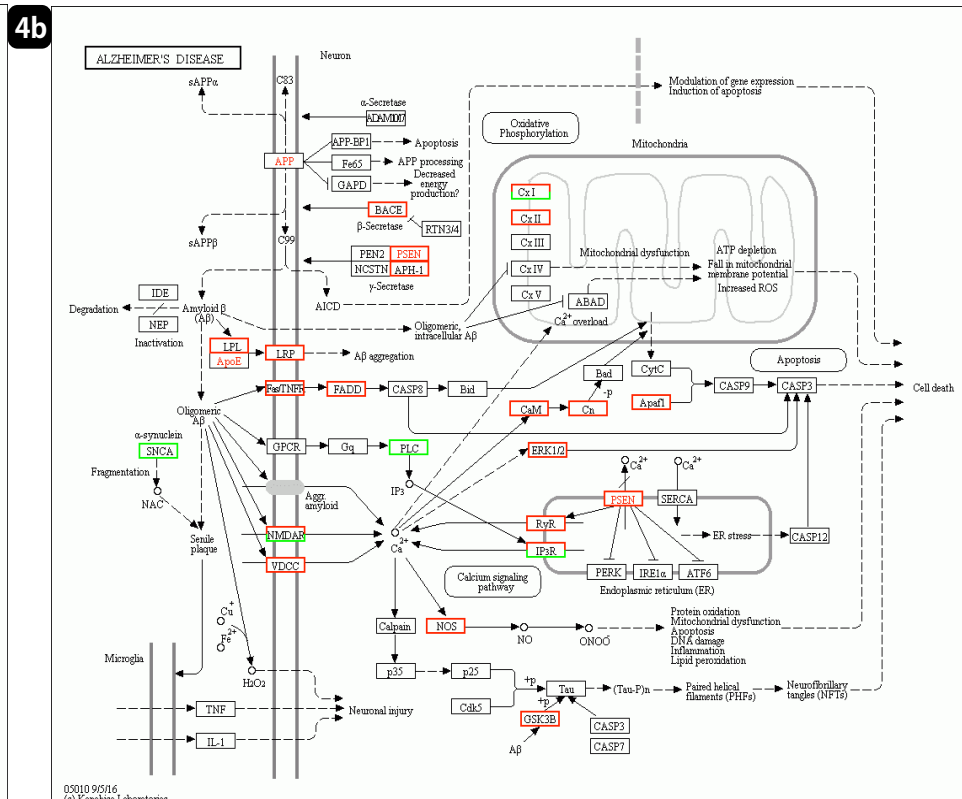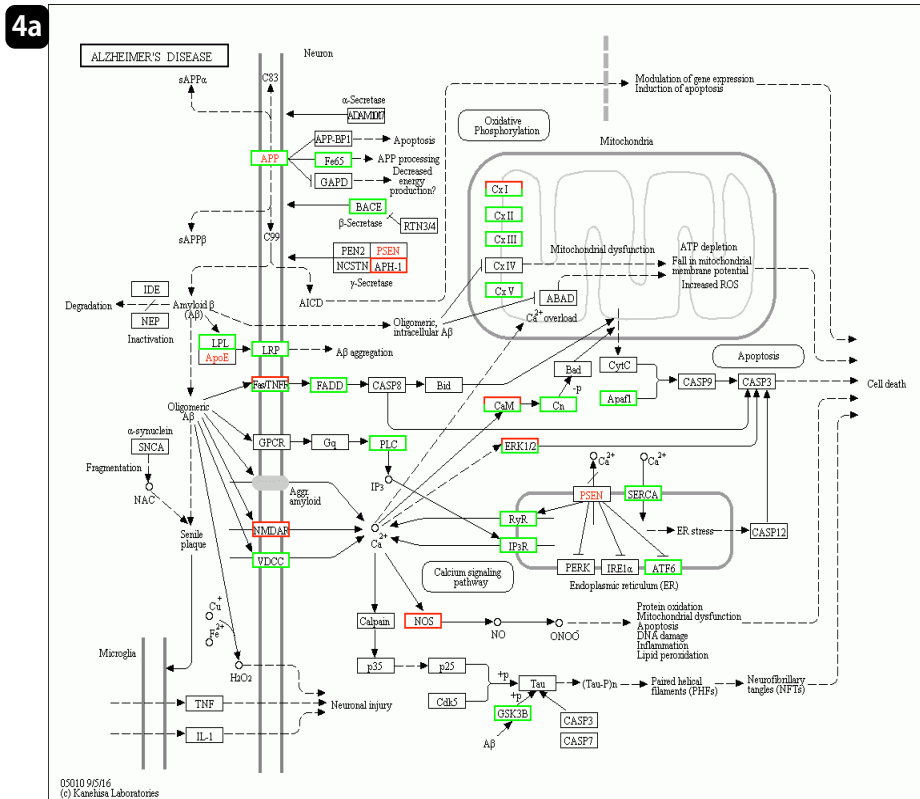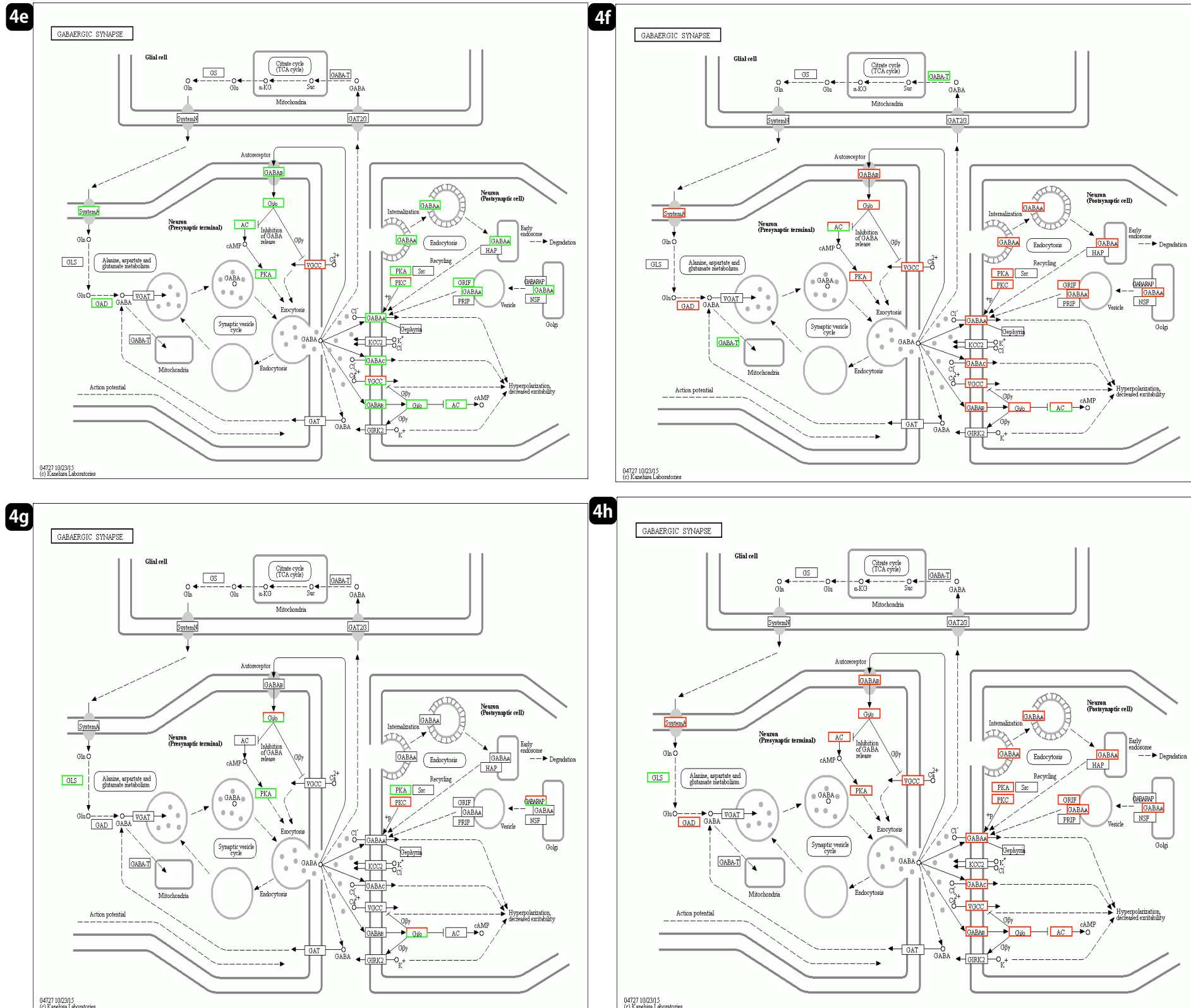
Figure 4: KEGG pathway analysis on lipid metabolism and inter/intra neural signal transfer. a-d: KEGG panel on lipid metabolism, e-h: KEGG panel on inter/intra neural signal transfer. a & d: patient No. 1; normal healthy control without Huaier administration. b & e: patient No. 2; normal healthy control with daily dose of Huaier 5g. c & f: patient No. 8; Stage IV oesophageral cancer, once successfully recovered, and relapse detected after 3rd shot of Pfizer-BioNTech vaccination. d & g: patient No.7; Stage IV lung adenocarcinoma, Huaier therapy 60g/day.

Figure 5: Comparison of the numbers of differentially expressed genes (DEGs) in each patient by time course of Pfizer-BioNTech vaccination. Upper: Statistics of miRNA, lower: piRNA.
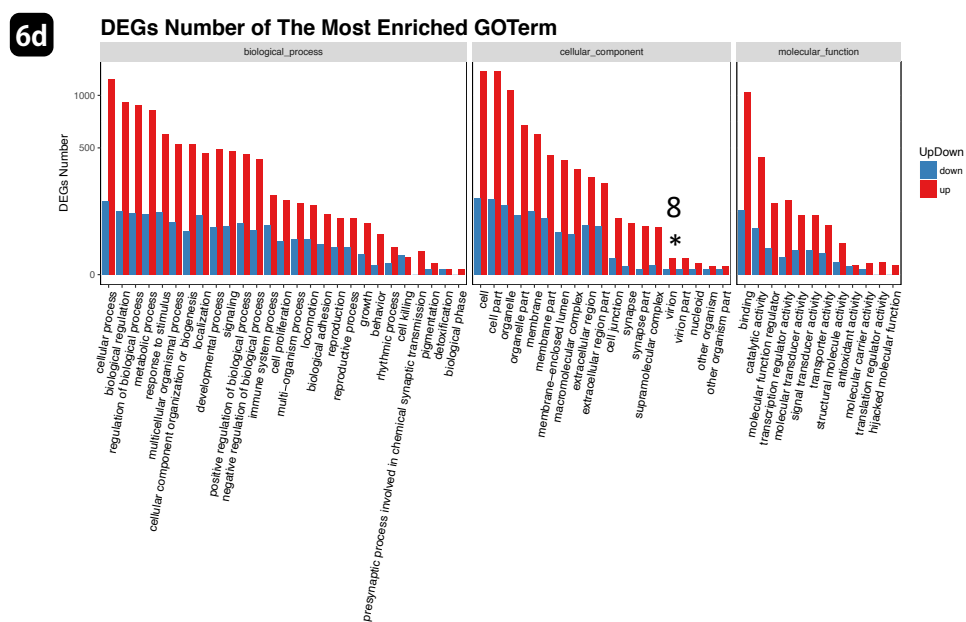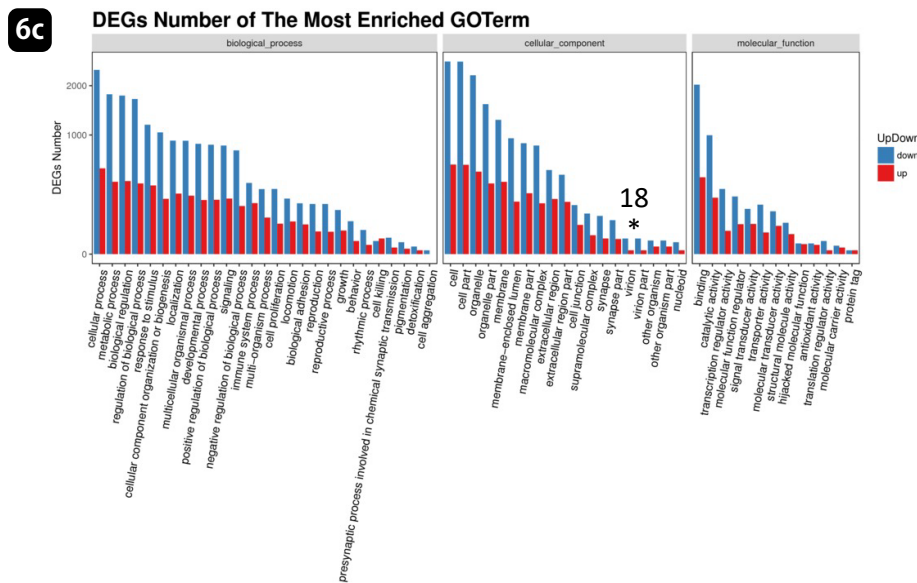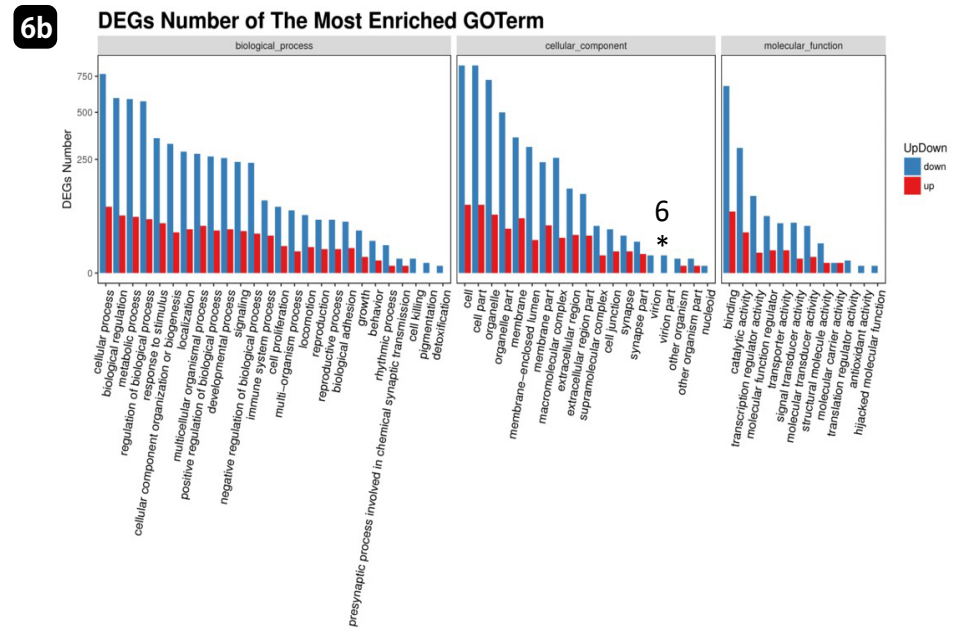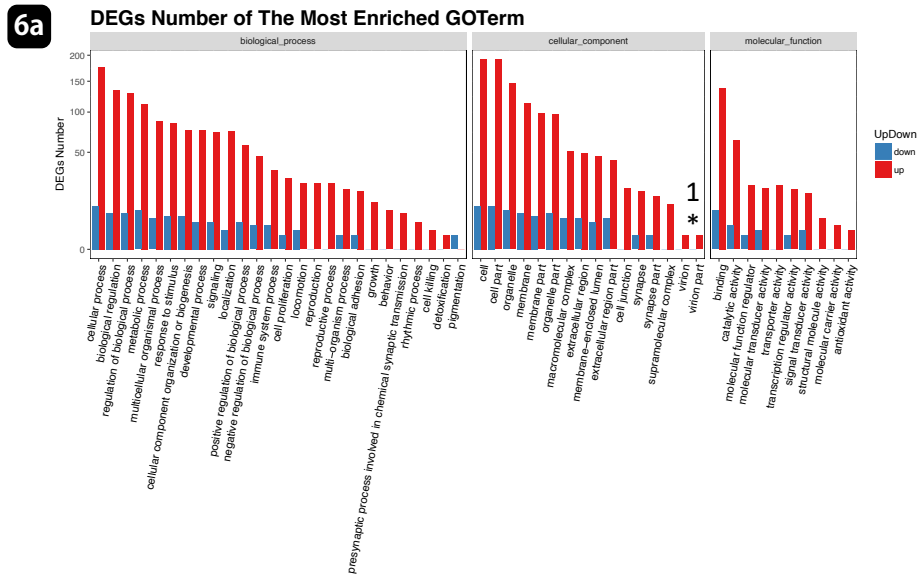
Figure 6: The enrichment pathways of regulation genes. The X axis is the terms of pathway, and the Y axis is the number of increased or decreased genes. The numbers of virion and virion part was indicated by * with numbers in each pane. The data of each patient at 3 months after Pfizer-BioNTech vaccination. a: patient No. 1; normal healthy control without Huaier administration. b: patient No. 2; normal healthy control with daily dose of Huaier 5g. c: patient No. 8; Stage IV oesophageal cancer, once successfully recovered, and relapse detected after 3rd shot of Pfizer-BioNTech vaccination. d: patient No.7; Stage IV lung adenocarcinoma, Huaier therapy 60g/day.

Citation: Manami Tanaka, Tomoo Tanaka, Xiaolong Zhu, Fei Teng, Hong Lin, Zhu Luo, Ying Pan, Sotaro Sadahiro, Toshiyuki Suzuki, Yuji Maeda, Ding Wei, Zhengxin Lu. Huaier Effects on Functional Compensation with Destructive Ribosomal RNA Structure after Anti-SARS-CoV-2 mRNA Vaccination. Archives of Clinical and Biomedical Research 6 (2022): 553-574.

Discussion

Thus, we have observed a significant quantitative and qualitative reaction of biological and physiological systems after the serial injections of Pfizer-BioNTech mRNA vaccine. Vaccination itself fulfilled its task to prevent COVID-19 infection [1-3], and the adjuvant therapy with Huaier (not specified Huaier only) succeeded to compensate the defects caused by destructive ribosomal RNA structures, by massive genomic flexibility and capability to manage Huaier effects as a kinase regulator [1, 12]. The compensation was well observed in alterations of transcriptional factors and linked DEGs, which resulted in the improvement of accelerated ageing process in lipid metabolism [11, 12], inter/intra neural signal transfer [9], and endocrine secretion systems, through activation of PI3K/AKT kinase-related signaling pathways. Considering inhibitory influence on DEG management by vaccination, minimum essential energy consumption was enough to this compensation.

In the former reports, we happened to observe the recovery process on the opportunistic virus infection in several patients [15], but the present study revealed spontaneous virion production after the viral mRNA injections. Although Huaier does not prevent or influence virus infection itself, the efficacy of Huaier observed can be speculated to control the latent damages of viral particle existence by down-regulation of production, and that with no correlations to the dose 3g to 60 g per day).

The world-wide struggle against COVID-19 focused on the prevention and acquisition of herd immunity among the large population [1-3]. The present study provides the other side of this strategy, how to survive the era after the present phase of pandemic. The data presented here advocates the requirement of some adjuvant therapy with vaccine strategy, not only by Huaier, to avoid the complications and influence of accelerated ageing by the infection [2], and also from vaccination.

It is emphasized here that even normal healthy person has a continuous influence by environmental stresses and infective agents, and physiological status is not so stable as we expect [6, 15]. The data here provides the proof of genomic potential can recover unstable genetic status in each person, and this potential for rescue and modulation in each individual is most important to the next stage of human history.

Ribosomal RNAs are essential components to all cells [41]. it makes up about 80% of cellular RNA despite never being translated into proteins itself. Ribosomal RNA genes have been found to be tolerant to modification and incursion. When ribosomal RNA sequencing is altered, cells have been found to become compromised and quickly cease normal function [42]. To produce rRNA, RNA polymerase I played a crucial role [43]. Synthesis of rRNA is up-regulated and down-regulated to maintain homeostasis by a variety of processes and interactions.

Ribosomal RNA is also the target of numerous clinically relevant antibiotics [44], however, the influence of mRNA vaccination itself has not yet been reported. According to this report, our first findings of low quality ribosomal RNAs should not have serious influence to homeostasis of the individuals.

Since ribosomal RNA is synthesized by RNA polymerase I, and together with the consideration of the fact that the genes for 5S rRNA are located inside the nucleolus and are transcribed into pre-5S rRNA by RNA polymerase III [45], we investigated KEGG analysis on these RNA polymerases and their interactions. However, no significant alterations were identified in those functions and related molecules.

The present study, however, provided evidence up-regulation of kinase AKT and its mediating activation of PI3K/AKT signaling pathway rescues any possible damages used by destructive ribosomal RNA structures observed after serial mRNA vaccination [46-49].

PI3K/AKT/mTOR pathway is an intracellular signaling pathway important in regulating the cell cycle. Therefore, it is directly related to cellular quiescence, proliferation, carcinogenesis, and longevity. TPI3K activation phosphorylates and activates kinase AKT [31]. AKT can have a number of downstream effects such as activating CREB [32], inhibiting p27 and p21 [33], for further transcription factor mediated functional control of the cells, and also activating mTOR signaling pathway [33]. There are many known factors that enhance the PI3K/AKT pathway including EGF [35], sonic hedgehog [32], IGF-1 [32], insulin [33], and CaM [34]. The pathway is antagonized by various factors including PTEN [36], GSK3B [32], and HB9 [35].

The maintenance and regulation of the factors written above were the symbolic findings in cancer patients who have recovered by Huaier therapy. These effects have been also suggested by the experiments using in vitro cultivated cancer cells [50, 51]. We have already provided the clue to the molecular basis of anti-cancer effects of Huaier, which plays a crucial role as a non-hazardous kinase regulator by series of publications [1, 12], and that the typical findings are to promote growth and proliferation over differentiation of stem cells specifically [32]. It is too difficult to find an appropriate balance the level of proliferation versus differentiation in the development of various therapies [32], we should emphasize that this pathway has been found to be a necessary component in neural long term potentiation [34, 46-49].

It can be speculated that this is the reason why Huaier could compensate for any damages from destructive ribosomal RNA structures, but at the same time, the extent of compensation depended on the genomic potential of each individual independent of the severity of cancer or basic health conditions. The accelerated ageing process in lipid metabolism has been observed, too.

Pfizer-BioNTech and Moderna vaccines contain mRNA that codes for the SARS-CoV-2 spike protein. The present study revealed that, when the vaccines are injected, they deliver the mRNA to cells, which make copies of not only expected spike, but also promotes spontaneous virion production. Normal individuals then clear the foreign genetic material within a few days, but those virions persisted for 3-6 months. Huaier administration induced significant down-regulation of those virion particles, not dependent on the dose of Huaier. It is reported self-amplifying vaccine will be introduced additional to the vaccine strategy against SARS-CoV-2, and others in development include enzymes from alphaviruses to repeatedly copy the genetic strand inside a cell and stay in the body for more than twice as long. An influence of self-amplifying mRNA COVID-19 [17] vaccine additional to the spontaneous copies of virion production remain unclear, and we need a scientific answer to the question that the novel type of vaccine ideally would replace the two primary doses, giving it an even clearer benefit over its conventional relatives.

Conclusion

Thus, the present study emphasizes the conclusion that the adjuvant therapy like Huaier, non-hazardous kinase regulator, is required together with vaccine strategy. Just recently many cases of microembolus are also being reported in the broadcast news in USA and Europe, and the solution should be provided.

Acknowledgements

Author contributions

T. T., M. T., designed the study from the clinical observation of the cancer patients with Huaier treatment (as a complementally therapy), and managed the sampling and clinical assessment of the patient volunteers, statistically analyzed the data, and drafted the manuscript. F. T., X. Z., H. L., Z. L., Y. P., managed total RNA and small nuclear RNA sequencing and conducted systematic analysis of the data. S. S., T. S., and Y. M., contributed clinical diagnosis and treatment of the patients, together with the assessment of QOL and the effects of Huaier administration, Z. L., D. W., contributed to the provision of Huaier granules and clinical evaluation of the data, especially focused on Immunological evaluation.

Competing interests

The authors declare no competing interests.

Data availability

The complete sequencing data of the cases have been deposited to NCBI database, and the clinical outcomes of these cases are not publicly available for data privacy but are available from Dr. Manami Tanaka (e-mail: tubu0125@gmail.com, manami-tanaka@bradeion.com) upon request for research collaboration. The timeframe for response to data access requests is 30 days. There are no restrictions on the reuse of data. In addition, the raw data of the longitudinal cohort and healthy individuals analyzed in this study were available at GEO with identifiers of NCBI GEO (GSE157086).

References

1. WHO. Coronavirus Situation Report (2021).

2. Cao X, Li W, Wang T, et al. Accelerated biological aging in COVID-19 patients. Nat Commun 13 (2022): 2135.

3. Chakraborty S, Mallajosyula V, Tato CM, et al. SARS-CoV-2 vaccines in advanced clinical trials: Where do we stand?. Adv Drug Deliv Rev 72 (2021): 314-338.

4. Fang E, Liu X, Li M, et al. Advances in COVID-19 mRNA vaccine development. Signal Transduct Target Ther 7 (2022): 94.

5. Indicators of Health Trends in National Health 2021/2022, Japan Health and Labor Statistics Association (2021).

6. Tanaka M, Tanaka T. Huaier Natural Herb Therapy for Cancer, Bradeion Institute of Medical Sciences Press (2022).

7. Tanaka M, Tanaka T, Teng F, et al. Biomedicine in 21st century: The practical health maintenance and successful recovery from cancer. J Biomed Biosens 1 (2021): 33-56.

8. Tanaka M, Tanaka T, Teng F, et al. Huaier therapy for successful recovery of cancer and health maintenance: Steady progress and the end of failed promise. Arch Clin Biomed Res 5 (2021): 457-483.

9. Tanaka M, Tanaka T, Teng F, et al. Huaier compensates impaired signal transfer inter/intra neurons in central and peripheral nervous systems. Arch Clin Biomed Res 5 (2021): 484-518.

10. Tanaka T, Tanaka M, Teng F, et al. Molecular basis of Huaier effects on immunomodulation, and natural selection of iPS cells with stable growth in vivo. J Pharm Res Dev (2021).

11. Tanaka M, Tanaka T, Teng F, et al. Huaier inhibits cancer progression and induces tissue regeneration by transcriptional regulation of pluripotency of stem cells. J Altern Compl Integr Med 7 (2021): 162-172.

12. Tanaka M, Tanaka T, Teng F, et al. Huaier inhibits cancer progression correlated with the mutated EGFR and other receptor tyrosine kinases (c-MET/erbB-2) by down-regulation of multiple signal transduction pathways. Arch Clin Biomed Res 5 (2021): 262-284.

13. Tanaka M, Tanaka T, Teng F, et al. Complete remission of the severe advanced stage cancer by miRNA-mediated transcriptional control of Bcl-xL with Huaier therapy compared to the conventional chemotherapy with platinum (II) complex. Arch Clin Biomed Res 5 (2021): 230-261.

14. Tanaka M, Tanaka T, Teng F, et al. Anti-cancer effects of Huaier on prostate cancer; miRNA-mediated transcription control induced both inhibition of active progression and prevention of relapse. J Altern Compl Integr Med 7 (2021): 146-155.

15. Tanaka M, Tanaka T, Teng F, et al. Huaier Induces Cancer Recovery by Rescuing Impaired Function of Transcription Control Based on the Individual Genomic Potential. Arch Clin Biomed Res 4 (2020): 817-855.

16. Tanaka T, Suzuki T, Nakamura J, et al. Huaier regulates cell fate by the rescue of disrupted transcription control in the Hippo signaling pathway. Arch. Clin. Biomed. Res 1 (2017): 179-199.

17. Cohen J. First self-copying mRNA vaccine proves itself in pandemic trial. Science 376 (2022): 6592.

18. Das M, Gursky O. Amyloid-Forming Proterties of Human Apolipoproteins: Sequence Analyses and Structural Insights. Adv Ex Med. Biol 855 (2015): 175-211.

19. Ren L, Yi J, Li W, et al. Apolipoproteins and cancer. Cancer Med 8 (2019): 7032-7043.

20. Zhu X, Wang Y, Nan J, et al. Comparative gene expression profiling and character development in stable angina pectoris disease. J Altern Compl Integr Med 7 (2021): 192.

21. Peng Z, Cheng Y, Tan BC, et al. Comprehensive analysis of RNA-Seq data reveals extensive RNA editing in a human transcriptome. Nat Biotechnol 30 (2012): 253-260.

22. Chen Y, Chen Y, Shi C, et al. SOAPnuke: a MapReduce acceleration-supported software for integrated quality control and preprocessing of high-throughput sequencing data. GigaScience 7 (2018): 1-6.

23. Li B, Dewey CL. RSEM: accurate transcript quantification from RNA-Seq data with or without a reference genome. BMC Bioinform 12 (2011): 323.

24. Love MI, Huber W, Anders S. Moderated estimation of fold change and dispersion for RNA-seq data with DESeq2. Genome Biol 15 (2014): 1-21.

25. Ben L, Salzberg SL. Fast gapped-read alignment with Bowtie 2. Nat Methods 9 (2012): 357-359.

26. Enright AJ, John B, Gaul U, et al. MicroRNA targets in Drosophila. Genome Biol 5 (2003): R1.

27. Agarwal V, Bell GW, Nam JW, et al. Predicting effective microRNA target sites in mammalian mRNAs. eLife 4 (2015): e05005.

28. Jiang Y, Sun A, ZhaoY, et al. Proteomics identifies new therapeutic targets of early-stage hepatocellular carcinoma. Nature 567 (2019): 257-261.

29. Song Y, Li L, Ou Y, et al. Identification of genomic alterations in oesophageal squamous cell cancer. Nature 509 (2014): 91-95.

30. Kanehisa M, Araki M, Goto S, et al. KEGG for linking genomes to life and the environment. Nucleic Acids Res 36 (2008): 480-484.

31. King D, Yeomanson D, Bryant HE. PI3King the lock: targeting the PI3K/Akt/mTOR pathway as a novel therapeutic strategy in neuroblastoma. J Pediatr Hematol Oncol 37 (2015): 245-251.

32. Peltier J, O'Neill A, Schaffer DV. PI3K/Akt and CREB regulate adult neural hippocampal progenitor proliferation and differentiation. Dev. Neurobiol 67 (2007): 1348-1361.

33. Rafalski VA, Brunet A. Energy metabolism in adult neural stem cell fate. Prog Neurobiol 93 (2011): 182-203.

34. Man HY, Wang Q, Lu WY, et al. Activation of PI3-kinase is required for AMPA receptor insertion during LTP of mEPSCs in cultured hippocampal neurons. Neuron 38 (2003): 611-624.

35. Ojeda L, Gao J, Hooten KG, et al. Critical role of PI3K/Akt/GSK3β in motoneuron specification from human neural stem cells in response to FGF2 and EGF. PLOS ONE 6 (2011): e23414.

36. Wyatt LA, Filbin MT, Keirstead HS. PTEN inhibition enhances neurite outgrowth in human embryonic stem cell-derived neuronal progenitor cells. J Comp Neurol 522 (2014): 2741-2755.

37. Morton Am, Koch M, Mendivil CO, et al. Apolipoproteins E and CIII interact to regulate HDL metabolism and coronary heart disease risk. JCI Insight 3 (2018): e98045.

38. Frank M Sacks. The crucial roles of apolipoproteins E and C-III in apoB lipoprotein metabolism in normolipidemia and hypertriglyceridemia. Curr Opin Lipidol 26 (2015): 56-63.

39. Yamazaki Y, Zhao N, Caulfield TR, et al. Apolipoprotein E and Alzheimer disease: pathobiology and targeting strategies. Nat Rev Neurol 15 (2019): 501-518.

40. Ju Son D. The atypical mechanosensitive microRNA-712 derived from pre-ribosomal RNA induces endothelial inflammation and atherosclerosis. Nat Commun 4 (2013): 3000.

41. Smit S, Widmann J, Knight R. Evolutionary rates vary among rRNA structural elements. Nucleic Acids Res 35 (2007): 3339-3354.

42. Ide S, Miyazaki T, Maki H, et al. Abundance of ribosomal RNA gene copies maintains genome integrity. Science 327 (2010): 693-696.

43. Engel C, Sainsbury S, Cheung AC, et al. RNA polymerase I structure and transcription regulation. Nature 502 (2013): 650-655.

44. Sloan KE, Warda AS, Sharma S, et al. Tuning the ribosome: The influence of rRNA modification on eukaryotic ribosome biogenesis and function. RNA Bio 14 (2017): 1138-1152.

45. Thompson M, Haeusler RA, Good PD, et al. Nucleolar clustering of dispersed tRNA genes. Science 302 (2003): 1399-1401.

46. Chan JC, Hannan KM, Riddell K, et al. AKT promotes rRNA synthesis and cooperates with c-MYC to stimulate ribosome biogenesis in cancer. Sci Signal 4 (2011): ra56.

47. Hoppe S, Bierhoff H, Cado I, et al. AMP-activated protein kinase adapts rRNA synthesis to cellular energy supply. Proc Natl Acad Sci USA 106 (2009): 17781-17786.

48. Liang XH, Liu Q, Fournier MJ. Loss of rRNA modifications in the decoding center of the ribosome impairs translation and strongly delays pre-rRNA processing. RNA 15 (2009): 1716-1728.

49. Brandman O, Hegde RS. Ribosome-associated protein quality control. Nat. Struct. Mol. Biol 23 (2016): 7-15.

50. Yan X, Lyu T, Jia N, et al. Huaier aqueous extract inhibits ovarian cancer cell motility via the AKT/GSK3beta/beta-catenin pathway. PLoS ONE 8 (2013): e63731.

51. Wang X, Qi W, Li Y, et al. Huaier extract induces autophagic cell death by inhibiting the mTOR/S6K pathway in breast cancer cells. PLoS ONE 10 (2015): e0131771.

Extended Table 1: Gene Expression summary identified in the present study.

Sample No.	Total clean reads	Total mapping ratio	Uniquely mapping ratio	Total gene number	Total transcript number
1-1	70,492,718	77.63	72.65	15,459	29,325
1-2	70,759,452	76.79	71.96	15,521	29,559
1-3	70,377,882	71.70	66.83	16,022	29,754
1-4	70,545,234	78.13	73.11	15,483	29,407
1-6	74,665,342	75.17	69.90	15,474	27,998
2-1	70,546,678	76.07	71.78	15,618	30,080
2-2	70,723,900	77.66	72.99	15,325	28,700
2-3	67,192,844	78.32	73.64	15,457	29,563
2-4	66,972,926	80.03	75.15	15,422	29,221
2-6	72,277,108	77.59	72.75	15,449	28,293
3-4	69,169,848	73.46	69.08	15,503	28,729
3-5	68,023,194	73.24	68.79	15,480	28,486
3-6	69,097,410	74.29	69.78	15,604	29,281
4-1	69,612,424	75.02	70.13	15,454	29,254
4-3	67,136,026	76.81	72.18	15,543	29,549
4-6	66,852,824	72.73	68.32	15,685	28,615
5-1	70,287,644	76.16	71.67	15,526	29,572
5-4	70,559,162	77.80	73.21	15,452	29,434
5-6	72,162,914	72.79	68.29	15,428	27,455
6-1	70,443,816	75.44	70.44	15,620	29,966
6-2	67,133,382	77.54	72.24	15,435	29,211
6-3	66,683,274	78.46	72.79	15,434	28,979
6-4	66,769,578	77.75	72.24	15,406	28,972
7-7	67,327,440	80.93	75.06	15,094	27,727
7-8	70,679,666	77.52	72.17	15,224	27,874
7-9	72,717,266	72.29	67.40	15,692	27,895
8-7	67,034,186	77.35	72.50	15,327	28,795
8-9	67,059,450	78.62	73.72	15,395	29,185
	Mean	**76.33**	71.46	15,483	**28,960**
	Max.	**80.93**	75.15	16,022	30,080
	Mini.	**71.70**	66.83	15,094	27,455

Citation: Manami Tanaka, Tomoo Tanaka, Xiaolong Zhu, Fei Teng, Hong Lin, Zhu Luo, Ying Pan, Sotaro Sadahiro, Toshiyuki Suzuki, Yuji Maeda, Ding Wei, Zhengxin Lu. Huaier Effects on Functional Compensation with Destructive Ribosomal RNA Structure after Anti-SARS-CoV-2 mRNA Vaccination. Archives of Clinical and Biomedical Research 6 (2022): 553-574.

Extended Table 2: The numbers of RNA editing events identified in each sample by splice event types.

Sample No.	A-G	C-T	Transition	A-C	A-T	C-G	G-T	Transversion	Total
1-1	36,435	36,711	73,146	6,182	3,959	8,708	6,426	25,275	98,421
1-2	36,967	37,118	74,085	6,275	4,016	8,972	6,329	25,592	99,677
1-3	52,668	52,960	105,628	10,453	7,247	12,851	10,788	41,339	146,967
1-4	37,726	37,716	75,442	6,358	4,107	8,950	6,447	25,862	101,304
1-6	31,168	31,152	62,320	5,312	3,426	7,419	5,500	21,657	83,977
2-1	40,030	39,670	79,700	6,895	4,519	9,625	6,986	28,025	107,725
2-2	31,754	31,859	63,613	5,327	3,383	7,541	5,409	21,660	85,273
2-3	36,986	36,525	73,511	6,311	3,957	8,773	6,406	25,447	98,958
2-4	32,833	32,597	65,430	5,621	3,472	7,893	5,612	22,598	88,028
2-6	29,203	29,264	58,467	5,233	3,304	7,117	5,361	21,015	79,482
3-4	34,536	34,085	68,621	5,966	4,037	8,460	6,133	24,596	93,217
3-5	34,497	34,441	68,938	5,954	4,016	8,380	6,148	24,498	93,436
3-6	35,738	35,701	71,439	6,282	4,119	8,853	6,356	25,610	97,049
4-1	41,196	41,458	82,654	6,947	4,594	9,650	7,008	28,199	110,853
4-3	39,022	39,118	78,140	6,669	4,353	9,385	6,770	27,177	105,317
4-6	35,228	35,232	70,460	6,324	4,058	8,621	6,234	25,237	95,697
5-1	36,549	36,543	73,092	6,283	3,948	8,779	6,254	25,264	98,356
5-4	36,691	36,844	73,535	6,285	3,885	8,741	6,327	25,238	98,773
5-6	29,073	29,219	58,292	5,077	3,224	6,815	5,036	20,152	78,444
6-1	44,891	44,913	89,804	7,564	4,889	10,602	7,514	30,569	120,373
6-2	38,087	38,646	76,733	6,419	4,055	9,065	6,349	25,888	102,621
6-3	37,347	37,525	74,872	6,089	3,820	8,684	6,168	24,761	99,633
6-4	36,861	37,278	74,139	6,172	3,912	8,719	6,271	25,074	99,213
7-7	28,605	28,704	57,309	4,787	3,080	6,803	4,963	19,633	76,942
7-8	27,809	27,996	55,805	4,770	2,974	6,555	4,740	19,039	74,844
7-9	34,269	34,167	68,436	7,000	5,025	8,366	7,115	27,506	95,942
8-7	33,036	33,216	66,252	5,594	3,615	8,044	5,740	22,993	89,245
8-9	34,586	34,417	69,003	5,781	3,717	8,298	6,025	23,821	92,824
Mean	35,850	35,896	71,745	6,212	4,025	8,595	6,301	25,133	96,878
Max.	52,668	52,960	105,628	10,453	7,247	12,851	10,788	41,339	146,967
Mini.	27,809	27,996	55,805	4,770	2,974	6,555	4,740	19,039	74,844
Total	1,003,791	10,05,075	2,008,866	173,930	112,711	240,669	176,415	703,725	2,712,591
% by total			74.1%		10.6%	15.4%		25.9%	

Citation: Manami Tanaka, Tomoo Tanaka, Xiaolong Zhu, Fei Teng, Hong Lin, Zhu Luo, Ying Pan, Sotaro Sadahiro, Toshiyuki Suzuki, Yuji Maeda, Ding Wei, Zhengxin Lu. Huaier Effects on Functional Compensation with Destructive Ribosomal RNA Structure after Anti-SARS-CoV-2 mRNA Vaccination. Archives of Clinical and Biomedical Research 6 (2022): 553-574.

Extended Table 3: The numbers of RNA editing events identified in each sample by SNP variation types.

Sample No.	Skipped exon	Mutually exclusive exon	Alternative 5' splicing site	Alternative 3' splicing site	Retained intron	Total
1-1	18,156	3,051	2,857	3,498	3,252	30,814
1-2	18,492	3,084	2,933	3,487	3,235	31,231
1-3	17,132	2,793	2,735	3,405	3,159	29,224
1-4	18,495	3,115	2,937	3,440	3,267	31,254
1-6	13,233	2,033	2,364	2,950	2,915	23,495
2-1	19,359	3,191	3,003	3,559	3,280	32,392
2-2	16,535	2,659	2,790	3,356	3,153	28,493
2-3	18,000	2,888	2,918	3,555	3,235	30,596
2-4	17,532	2,903	2,891	3,468	3,244	30,038
2-6	13,874	2,140	2,451	3,039	2,954	24,458
3-4	14,528	2,102	2,555	3,131	2,985	25,301
3-5	14,439	2,223	2,466	3,049	2,953	25,130
3-6	16,000	2,442	2,672	3,307	3,094	27,515
4-1	17,986	2,996	2,812	3,394	3,232	30,420
4-3	18,940	3,124	2,985	3,495	3,271	31,815
4-6	14,641	2,283	2,459	3,050	2,975	25,408
5-1	18,322	2,994	2,904	3,481	3,216	30,917
5-4	18,513	3,001	2,928	3,500	3,270	31,212
5-6	**11,648**	**1,704**	**2,156**	**2,756**	**2,813**	21,077
6-1	**20,222**	**3,368**	**2,954**	**3,567**	**3,311**	33,422
6-2	17,917	2,895	2,886	3,431	3,234	30,363
6-3	17,895	2,952	2,786	3,375	3,196	30,204
6-4	17,893	2,993	2,776	3,395	3,170	30,227
7-7	15,463	2,631	2,591	3,149	3,076	26,910
7-8	15,001	2,450	2,495	3,078	3,092	26,116
7-9	12,723	1,913	2,203	2,849	**2,809**	22,497
8-7	17,069	2,736	2,791	3,304	3,204	29,104
8-9	17,869	2,930	2,852	3,443	3,202	30,296
Mean	**16,710**	**2,700**	**2,720**	**3,304**	**3,136**	28,569
Max.	**20,222**	**3,368**	**3,003**	**3,567**	**3,311**	20,222
Mini.	**11,648**	**1,704**	**2,156**	**2,756**	**2,809**	1,704
Total	467,877	75,594	76,150	92,511	87,797	799,929
Each AS/Total	58.5%	9.5%	9.5%	11.6%	11.0%	

Citation: Manami Tanaka, Tomoo Tanaka, Xiaolong Zhu, Fei Teng, Hong Lin, Zhu Luo, Ying Pan, Sotaro Sadahiro, Toshiyuki Suzuki, Yuji Maeda, Ding Wei, Zhengxin Lu. Huaier Effects on Functional Compensation with Destructive Ribosomal RNA Structure after Anti-SARS-CoV-2 mRNA Vaccination. Archives of Clinical and Biomedical Research 6 (2022): 553-574.

Extended Table 4: The numbers of up- and down- regulated differentially expressed genes (DEGs) in each patient by the time course of sampling according to the Pfizer-BioNTech vaccination.

Comparison No.	Up-regulated	Down-regulated
1-1-vs-1-2	44	10
1-1-vs-1-3	274	19
1-1-vs-1-4	34	18
1-1-vs-1-6	297	351
1-2-vs-1-3	244	20
1-2-vs-1-4	9	20
1-2-vs-1-6	278	582
1-3-vs-1-4	21	241
1-3-vs-1-6	291	606
1-4-vs-1-6	305	507
2-1-vs-2-2	124	**1,095**
2-1-vs-2-3	12	41
2-1-vs-2-4	22	323
2-1-vs-2-6	238	772
2-2-vs-2-3	192	233
2-2-vs-2-4	33	47
2-2-vs-2-6	882	330
2-3-vs-2-4	69	18
2-3-vs-2-6	236	236
2-4-vs-2-6	463	306
3-4-vs-3-5	35	55
3-4-vs-3-6	23	48
3-5-vs-3-6	36	27
4-1-vs-4-3	226	106
4-1-vs-4-6	560	320
4-3-vs-4-6	349	300
5-1-vs-5-4	25	32
5-1-vs-5-6	601	333
5-4-vs-5-6	568	237
6-1-vs-6-2	133	287
6-1-vs-6-3	25	273
6-1-vs-6-4	113	432
6-2-vs-6-3	17	73
6-2-vs-6-4	29	46
6-3-vs-6-4	40	25
7-7-vs-7-8	331	313
7-7-vs-7-9	**1,712**	242
7-8-vs-7-9	1,618	295
8-7-vs-8-9	29	**5**
Mean	**270**	**237**
Max.	**1,712**	**1,095**
Mini.	**9**	**5**
Subtotal	10,538	9,224
Total	**19,762**	

Citation: Manami Tanaka, Tomoo Tanaka, Xiaolong Zhu, Fei Teng, Hong Lin, Zhu Luo, Ying Pan, Sotaro Sadahiro, Toshiyuki Suzuki, Yuji Maeda, Ding Wei, Zhengxin Lu. Huaier Effects on Functional Compensation with Destructive Ribosomal RNA Structure after Anti-SARS-CoV-2 mRNA Vaccination. Archives of Clinical and Biomedical Research 6 (2022): 553-574.

Extended Table 5: The numbers of detected known and novel small non-coding RNA counts.

Sample No.	Known miRNA count	Novel miRNA count	Known piRNA count	Novel piRNA count
1-1	624	12	38	23
1-2	634	17	27	18
1-3	603	13	23	25
1-4	526	10	19	19
1-6	575	7	65	10
2-1	598	15	30	19
2-2	694	23	23	30
2-3	585	11	32	20
2-4	591	17	30	20
2-6	509	2	86	6
3-4	488	5	61	4
3-5	538	7	68	5
3-6	461	3	45	2
4-1	650	11	42	16
4-3	573	9	20	26
4-6	524	5	61	6
5-1	662	14	23	26
5-4	678	25	43	31
5-6	502	2	63	2
6-1	588	8	46	6
6-2	601	18	12	23
6-3	553	11	16	15
6-4	639	17	26	32
7-7	698	19	46	30
7-8	730	26	26	37
7-9	645	10	67	13
8-7	666	17	36	26
8-9	617	13	27	16
Mean	598	12	40	18
Max.	730	26	86	37
Mini.	461	2	12	2

Citation: Manami Tanaka, Tomoo Tanaka, Xiaolong Zhu, Fei Teng, Hong Lin, Zhu Luo, Ying Pan, Sotaro Sadahiro, Toshiyuki Suzuki, Yuji Maeda, Ding Wei, Zhengxin Lu. Huaier Effects on Functional Compensation with Destructive Ribosomal RNA Structure after Anti-SARS-CoV-2 mRNA Vaccination. Archives of Clinical and Biomedical Research 6 (2022): 553-574.

Extended Table 6: The numbers of up- and down-regulation sRNAs by the time course of Pfizer-BioNTech mRNA vaccination.

Comparison No.	Up-regulated miRNA	Down-regulated miRNA	Up-regulated piRNA	Down-regulated piRNA
1-1-vs-1-2	13	15	0	1
1-1-vs-1-3	13	11	0	1
1-1-vs-1-4	7	50	0	3
1-1-vs-1-6	18	95	0	3
1-2-vs-1-3	12	4	0	0
1-2-vs-1-4	7	42	0	1
1-2-vs-1-6	5	97	1	3
1-3-vs-1-4	2	42	0	2
1-3-vs-1-6	8	109	1	2
1-4-vs-1-6	27	73	1	1
2-1-vs-2-2	98	5	2	0
2-1-vs-2-3	34	13	2	0
2-1-vs-2-4	47	19	1	0
2-1-vs-2-6	9	158	7	2
2-2-vs-2-3	9	71	0	2
2-2-vs-2-4	10	67	0	2
2-2-vs-2-6	5	244	5	3
2-3-vs-2-4	20	15	0	0
2-3-vs-2-6	10	186	4	2
2-4-vs-2-6	6	194	5	2
3-4-vs-3-5	11	13	0	1
3-4-vs-3-6	4	69	0	4
3-5-vs-3-6	5	67	0	3
4-1-vs-4-3	13	36	0	8
4-1-vs-4-6	8	193	1	3
4-3-vs-4-6	9	146	5	1
5-1-vs-5-4	14	19	1	1
5-1-vs-5-6	3	184	2	3
5-4-vs-5-6	5	193	2	3
6-1-vs-6-2	78	1	0	4
6-1-vs-6-3	77	10	0	1
6-1-vs-6-4	80	1	1	3
6-2-vs-6-3	6	14	1	0
6-2-vs-6-4	8	5	1	0
6-3-vs-6-4	19	7	0	0
7-7-vs-7-8	57	4	0	1
7-7-vs-7-9	7	122	3	3
7-8-vs-7-9	8	197	3	3
8-7-vs-8-9	3	16	0	2
Mean	20	72	1	2
Max.	98	244	7	8
Mini.	2	1	0	0

Citation: Manami Tanaka, Tomoo Tanaka, Xiaolong Zhu, Fei Teng, Hong Lin, Zhu Luo, Ying Pan, Sotaro Sadahiro, Toshiyuki Suzuki, Yuji Maeda, Ding Wei, Zhengxin Lu. Huaier Effects on Functional Compensation with Destructive Ribosomal RNA Structure after Anti-SARS-CoV-2 mRNA Vaccination. Archives of Clinical and Biomedical Research 6 (2022): 553-574.